

# ECOS 2026: Potential of the adsorption performance of food-industry waste gasification residues for environmental pollutant removal

*Aneta Magdziarz<sup>a</sup>, Agata Stempkowska<sup>b</sup>, Monika Orlof-Naturalna<sup>b</sup>,  
Agata Mlonka-Mędrala<sup>c</sup>, Małgorzata Cierpińska<sup>a</sup>, and Wojciech Jerzak<sup>a</sup>*

<sup>a</sup> AGH University of Krakow, Faculty of Metals Engineering and Industrial Computer Science,  
Department of Heat Engineering & Environment Protection, Krakow, Poland,  
amagdzia@agh.edu.pl (CA), msieradz@agh.edu.pl, wjerzak@agh.edu.pl

<sup>b</sup> AGH University of Krakow, Faculty of Civil Engineering and Resources Management, Department  
of Environmental Engineering, Krakow, Poland, stemp@agh.edu.pl, orlof@agh.edu.pl

<sup>c</sup> AGH University of Krakow, Faculty of Energy and Fuels, Department of Thermal and Flow Machines,  
Krakow, Poland, amlonka@agh.edu.pl

## Abstract:

Agro-food processing residues are promising feedstocks for thermochemical valorisation because they are abundant, carbon-rich, and can be converted into energy carriers and functional carbon-based materials. Gasification is an attractive thermochemical route that enables the production of hydrogen-rich syngas along with a solid carbonaceous residue, biochar. The results of gasification under steam-enriched conditions promoted pore development and yielded biochar with highly developed specific surface areas, particularly for sunflower husk materials.

In this study, biochars obtained by gasifying sunflower husks and cherry seeds in CO<sub>2</sub> and CO<sub>2</sub> + H<sub>2</sub>O (steam) atmospheres were evaluated as adsorbents for the removal of phenol and Pb<sup>2+</sup> ions from water. Residual phenol concentration was determined by the UV–VIS method, while Pb<sup>2+</sup> was quantified by an ion-selective electrode and verified by atomic absorption spectrometry (ASA). The results demonstrated that phenol adsorption strongly depended on the feedstock type and gasification conditions. The sunflower husk biochar showed the highest phenol uptake, exceeding 11 mg/g at an initial phenol concentration of 50 mg/dm<sup>3</sup>, with the best performance observed for the CO<sub>2</sub>-activated sample. In contrast, cherry seed biochar exhibited lower adsorption capacity. The adsorption data were best fitted by the Freundlich model, indicating surface heterogeneity and a predominantly physical adsorption mechanism. These suggest that adsorption efficiency was governed not only by surface area, but also by pore structure and surface chemistry. For Pb<sup>2+</sup> removal, biochars from sunflower hulls showed nearly complete adsorption efficiency in the range 50–150 mg/dm<sup>3</sup>. Cherry-seed biochar was less effective, with sorption efficiency decreasing from 91.3% to 71.6% as the initial Pb<sup>2+</sup> concentration increased. Changes in pH and conductivity after sorption suggested that different uptake mechanisms depended on the precursor type. These findings confirm that gasification-derived biochars from selected food-industry wastes can serve as effective, low-cost sorbents for the removal of phenol and Pb<sup>2+</sup> ions.

## Keywords:

Food-industry waste; Gasification; Biochar; Adsorption properties.

## 1. Introduction

The growing contamination of water resources by industrial and agro-industrial effluents has intensified the research for efficient, low-cost, and sustainable adsorbent materials. Among the available options, biochar has attracted increasing attention because it can be produced from a wide range of biomass waste and converted into a functional carbon material with environmental applications [1,2]. Depending on the feedstock and thermochemical processing conditions, biochar may exhibit a well-developed porous structure, a high specific surface area, aromatic carbon domains, mineral phases, and a variety of oxygen-containing surface groups, all of which are relevant to adsorption [1–3]. These properties determine not only the overall adsorption capacity, but also the dominant removal mechanisms, which may include pore filling, physical adsorption, electrostatic attraction, ion exchange, surface complexation, hydrogen bonding, and π–π interactions [1,2,4].

Consequently, the adsorption performance of biochar is highly sensitive to its origin and production route, and even materials derived from apparently similar biomasses may behave differently toward specific pollutants [1,2].

A major advantage of biochar lies in the possibility of valorising agricultural and food-industry by-products that would otherwise remain underutilised or require disposal. This feature makes biochar particularly relevant within circular-economy strategies, where low-value residues are transformed into adsorbents, catalysts, soil amendments, or carbon-sequestration materials [2,5]. Recent research shows that the environmental relevance of waste-derived biochar extends beyond simple pollutant uptake: such materials may reduce treatment costs, decrease greenhouse-gas emissions when replace conventional adsorbents, and support integrated waste-to-resource approaches [5,6]. At the same time, it has become increasingly clear that the adsorption efficiency of biochar cannot be explained solely by its surface area. The size and connectivity of pores, degree of aromatic condensation, abundance of defects, mineral matter content, and distribution of surface functionalities all contribute to the final affinity toward contaminants [1,2,7]. This is especially important when comparing the removal of organic aromatic molecules with the uptake of hydrated metal ions, since the two pollutant groups interact with carbon materials through different, often overlapping, mechanisms [1,2].

Phenolic compounds are among the most common and hazardous organic pollutants in wastewaters. They occur in effluents from petroleum refining, pharmaceuticals, mining, metal treatment, resin manufacturing, coking, and pulp-related industries, and may exert toxic effects even at relatively low concentrations [3,8,9]. Phenol is therefore widely used as a model pollutant in studies on adsorbent performance. Although biological oxidation, chemical oxidation, membrane separation, and advanced oxidation processes have all been proposed for phenol removal, adsorption remains one of the most practical approaches because of its operational simplicity, relatively low cost, and applicability over a broad concentration range [3,8]. The effectiveness of phenol adsorption on biochar is strongly influenced by the microstructure and surface chemistry of the sorbent. Recent studies show that enhanced phenol removal is associated with the development of microporosity, high aromaticity, suitable hydrophobicity, and the presence of active sites capable of donor–acceptor or hydrogen-bonding interactions [10]. In engineered biochars, additional heteroatoms or metal-containing sites may further improve phenol uptake, but even non-modified lignocellulosic biochars may display significant sorption potential when their carbon structure and pore system are favourable [3,9]. Furthermore, the reactivity of biochar toward phenolic pollutants does not always involve simple adsorption alone. Surface-mediated polymerization or oxidative transformation may also occur under certain conditions, indicating that the role of biochar in phenol removal may be more complex than direct physical uptake [8].

Inorganic contamination is another major challenge to water protection, especially for heavy metals, which are persistent, non-biodegradable, and prone to accumulation in environmental compartments. Among them, lead is of particular concern due to its widespread occurrence, toxicity, and tendency to persist in soils and waters [1,2]. Lead contamination is associated with mining, metallurgy, battery production, electroplating, pigment production, and various historical industrial practices. Its adverse effects on human health include damage to the nervous, digestive, cardiovascular, and renal systems, and the risk is especially important because lead is poorly metabolised in the human body [1,2]. For this reason, efficient methods for  $Pb^{2+}$  removal remain a priority. Conventional methods include chemical precipitation, membrane filtration, ion exchange, and electrochemical treatment; however, these techniques may involve high operating costs, secondary waste generation, or limited effectiveness under some conditions [1]. Adsorption is therefore regarded as one of the most promising alternatives, particularly when low-cost sorbents are available [1,2]. Biochar is especially attractive in this context because it may bind  $Pb^{2+}$  through a combination of electrostatic attraction, ion exchange, surface complexation by oxygen-containing groups, interactions with ash-derived mineral phases, and precipitation phenomena [11]. The relative importance of these mechanisms depends on both solution chemistry and the composition of the biochar matrix. Consequently, feedstock-specific inorganic composition and thermochemical history may critically determine the efficiency of  $Pb^{2+}$  sorption [12].

Although the literature on pollutant removal by biochar is extensive, many studies focus on pyrolysis-derived materials or chemically modified and composite biochars designed for specific applications [3,4,11]. Comparatively less attention has been paid to chars obtained as solid residues from gasification, even though gasification is highly relevant to integrated waste valorisation. In such systems, the process may simultaneously yield a useful gaseous fuel and a porous carbonaceous residue with potential adsorptive properties. This is particularly important for residues from the food-processing industry, which are abundant, inexpensive, and lignocellulosic in nature [5]. Sunflower husks and cherry stones are promising examples of such feedstocks because they are carbon-rich by-products that differ in biochemical and mineral composition, and these differences may strongly affect the structure, surface chemistry, and adsorption behaviour of the resulting chars [5]. Previous work on these materials demonstrated that gasification under  $CO_2$  and steam-enriched  $CO_2$  atmospheres can substantially modify the textural properties of the obtained chars, especially by enhancing porosity and specific surface area [5, 13]. Such observations suggest that gasification-derived

biochars from agro-food residues may be promising sorbents for both organic and inorganic pollutants, but their adsorption performance still requires systematic evaluation.

Therefore, the aim of this study was to investigate the adsorption properties of biochars obtained as solid residues from the gasification of selected food-industry wastes, namely sunflower husks and cherry stones, under CO<sub>2</sub> and CO<sub>2</sub> + H<sub>2</sub>O atmospheres. The sorption performance of these materials was evaluated toward two model pollutants representing distinct contaminant classes: phenol as a toxic organic compound and Pb<sup>2+</sup> as a hazardous heavy metal ion. By linking adsorption behaviour with feedstock type and gasification atmosphere, this work contributes to the development of low-cost bio-based sorbents and to the broader valorisation of food-processing residues within sustainable environmental technologies.

## 2. Materials and methods

### 2.1. Materials

The feedstocks used in this study were sunflower husks (SH) and cherry stones (CS), both of which are abundant lignocellulosic by-products generated by the food-processing industry and therefore qualify as food-industry waste. These materials were selected because they are readily available, carbon-rich, and suitable for thermochemical valorisation into functional carbon materials. In addition to their practical relevance as agro-food residues, sunflower husks and cherry stones differ in their biochemical composition, making them suitable model feedstocks for evaluating how raw material properties influence the characteristics of gasification-derived biochars.

Cherry stones are characterised by relatively high carbon and hydrogen contents, high volatile matter, and low ash content, making them a promising feedstock for forming carbon-rich solid residues during thermochemical conversion. They are also reported to contain a relatively high lipid fraction and elevated nitrogen content compared with the other investigated food wastes, which may affect both carbonisation behaviour and the chemical nature of the resulting biochar surface. In contrast, sunflower husks also exhibit high volatile matter and moderate ash content, but they are distinguished by a higher contribution of hemicellulose and a mineral fraction rich in alkali and alkaline earth elements, especially potassium and calcium. Such differences in organic and inorganic composition may significantly affect gasification reactivity, pore development, ash behaviour, and the final adsorption properties of the biochars. The details of the physical and chemical properties of these feedstocks and the obtained biochars were presented in the authors' previous paper [5].

The biochars were obtained as solid residues from the gasification process conducted in a laboratory-scale vertical fixed-bed reactor at 900 °C. The materials were converted under two atmospheres: pure CO<sub>2</sub> and steam-enriched CO<sub>2</sub> (CO<sub>2</sub> + H<sub>2</sub>O). The present work focuses on the adsorption properties of the solid residues (biochar) produced by gasification. Detailed data concerning the gasification process, including the composition of the gaseous products, are presented in a separate publication [13].

### 2.2. Methods

Phenol adsorption experiments were carried out in 250 cm<sup>3</sup> Erlenmeyer flasks. A mass of 0.2 g of adsorbent was accurately weighed using an analytical balance (Ohaus, accuracy ±0.0001 g) and mixed with 100 mL of phenol solutions with initial concentrations of 5, 10, 25, and 50 mg/dm<sup>3</sup>.

A stock solution of phenol with a concentration of 1000 mg/dm<sup>3</sup> was prepared by dissolving an appropriate amount of phenol (analytical grade) in demineralized water (pH ≈ 6.57). Working solutions were obtained by appropriate dilution of the stock solution. The mixtures were agitated for 60 min using a laboratory shaker (SK-0330 PRO, DragonLab Instruments) at a constant speed of 210 rpm. The contact time was selected based on preliminary experiments as sufficient to reach adsorption equilibrium. The process was conducted at room temperature (approximately 22 °C).

After the adsorption process, the suspensions were separated by gravitational filtration. The residual phenol concentration was determined using the 4-aminoantipyrine (4-AAP) colorimetric method. In alkaline conditions (pH ≈ 10), phenol reacts with 4-aminoantipyrine in the presence of an oxidizing agent (potassium ferricyanide) to form a red-colored antipyrine dye.

The absorbance of the formed complex was measured using a UV–VIS spectrophotometer (NANOCOLOR UV–VIS II, Macherey-Nagel) at a wavelength of approximately 510 nm.

The equilibrium adsorption capacity ( $q_e$ ) was calculated based on the difference between the initial and equilibrium phenol concentrations.

The pH of the solutions was measured before and after the adsorption process using a pH meter manufactured by Mettler Toledo. All measurements were carried out at room temperature (approximately 22 °C). The pH values were recorded to assess changes in solution chemistry upon contact with the biochar and to support the interpretation of potential adsorption mechanisms.

The textural properties of the biochars derived from sunflower husk and cherry stone biochars were determined by low-temperature nitrogen adsorption–desorption measurements using an Anton Paar NOVA 800 surface area and pore size analyser. The adsorption isotherms were recorded at 77.35 K using nitrogen as the adsorbate. Prior to analysis, the samples were placed in 9 mm cells with a filler rod and degassed under vacuum to remove physically adsorbed moisture and volatile impurities. The degassing process was carried out at 350 °C with a heating rate of 5 °C/min, followed by an isothermal hold of 1200 min. Helium was used to determine the void volume before the adsorption measurement.

### Phenol adsorption isotherm models

The adsorption equilibrium was interpreted using several commonly applied isotherm models, including Freundlich, Langmuir, Temkin, and Dubinin-Radushkevich. Each of these models provides different assumptions regarding the nature of the adsorbent surface and the adsorption mechanism. The Freundlich isotherm is an empirical model describing adsorption on energetically heterogeneous surfaces. It assumes a non-uniform distribution of adsorption heat and affinities over the surface, allowing for multilayer adsorption. This model is particularly suitable for systems where surface heterogeneity plays a significant role. The logarithmic form of the equation of the Freundlich model (1) is described as follows:

$$\log q_e = \log K_f + \left(\frac{1}{n}\right) \log C_e \quad (1)$$

where the adsorption capacity at equilibrium ( $q_e$ ) expressed in mg/g represents the amount of phenol adsorbed per unit mass of adsorbent under equilibrium conditions. The equilibrium concentration ( $C_e$ ), given in mg/L, corresponds to the concentration of phenol remaining in the solution after the adsorption process reaches equilibrium. The Freundlich constant ( $K_f$ ) is related to the adsorption capacity of the adsorbent, while the parameter  $n$  describes the adsorption intensity and surface heterogeneity of the adsorbent

In contrast, the Langmuir isotherm assumes that adsorption occurs on a homogeneous surface with a finite number of identical and energetically equivalent active sites. It describes monolayer adsorption without interactions between adsorbed molecules and is often used to estimate the adsorbent's maximum adsorption capacity.

The linearised form of the Langmuir equation (2) is expressed as follows:

$$\frac{C_e}{q_e} = \frac{C_e}{q_m} + \frac{1}{K_L q_m} \quad (2)$$

where adsorption capacity ( $q_e$ ), expressed in mg/g, represents the amount of adsorbate retained per unit mass of adsorbent at equilibrium. The equilibrium concentration ( $C_e$ ), given in mg/dm<sup>3</sup>, corresponds to the concentration of the adsorbate remaining in the solution after equilibrium is reached. The maximum adsorption capacity ( $q_m$ ), expressed in mg/g, indicates the theoretical monolayer capacity of the adsorbent surface. The Langmuir constant ( $K_L$ ), given in dm<sup>3</sup>/mg, is related to the affinity between the adsorbate and the adsorbent and reflects the energy of adsorption.

The Temkin isotherm accounts for interactions between the adsorbate and the adsorbent. It assumes that the heat of adsorption decreases linearly with increasing surface coverage due to these interactions, making it useful for describing systems where adsorbate-adsorbent interactions are significant.

Temkin isotherm has the linear forms as follows (3,4):

$$q_e = B \ln K_t + B \ln C_e \quad (3)$$

$$B = \frac{RT}{b_t} \quad (4)$$

The adsorption capacity ( $q_e$ ), expressed in mg/g, represents the amount of adsorbate retained per unit mass of adsorbent at equilibrium. The equilibrium concentration ( $C_e$ ), given in mg/dm<sup>3</sup>, corresponds to the concentration of the adsorbate remaining in the solution after equilibrium is reached. The Temkin constant ( $K_t$ ) is related to the binding equilibrium, while the constant  $B$  is associated with the heat of adsorption. The parameter  $R$  denotes the universal gas constant (8.314 J/mol ·K), and  $T$  represents the absolute temperature in Kelvin. The constant  $b_t$  is the Temkin energy constant, related to the variation of adsorption energy.

The Dubinin-Radushkevich (D-R) isotherm is a more general empirical model that does not assume a homogeneous surface or constant adsorption potential. It is commonly applied to distinguish between physical and chemical adsorption processes based on the calculated mean adsorption energy.

Dubinin-Radushkevich model were calculated from the following equations (5,6):

$$\ln q_e = \ln q_m - K_{DR} \varepsilon^2 \quad (5)$$

$$\varepsilon = RT \ln \left( 1 + \frac{1}{c_e} \right) \quad (6)$$

where adsorption capacity at equilibrium ( $q_e$ ) and the maximum adsorption capacity ( $q_m$ ), both expressed in mg/g, describe the amount of adsorbate retained per unit mass of adsorbent. The constant  $K_{DR}$  is related to the adsorption energy and is used to estimate the nature of the adsorption process.

The linear forms of the applied isotherm models were used to evaluate the adsorption parameters and to determine the best-fitting model for the experimental data.

### Lead adsorption isotherm models

The adsorption of  $Pb^{2+}$  was investigated analytically. For these experiments, 250 cm<sup>3</sup> conical flasks were used. The tests used 0.2 g of biochar sorbents, measured on an analytical balance with an accuracy of 0.0001 g, and 100 ml of lead ion solutions with initial concentrations of 50, 100, and 150 mg/dm<sup>3</sup>. The base solutions used for adsorption, each 100 ml, contained lead ions at initial concentrations of 50, 100, and 150 mg/dm<sup>3</sup>. The solutions were prepared by appropriately diluting a basic solution of  $Pb^{2+}$  ions at 1 g/ml. This solution was prepared from anhydrous lead (II) nitrate (V),  $Pb(NO_3)_2$ , with a purity of p.a. (*Chempur*), weighing the appropriate amount on an analytical balance with an accuracy of 0.0001g (*Ohaus*).

All solutions were prepared in water obtained from a Hydrolab device (demineralized water – third degree of purification according to PN-EN ISO 3696:1999 – pH = 6.29, conductivity approx. 3 μS/cm). The solutions in the flasks were shaken for 60 min on a laboratory shaker SK-0330 PRO at a speed of 210 rpm (*DragonLab Instruments*). The length of the process was determined on the basis of previous studies. It was assumed that 60 min was sufficient to reach sorption equilibrium. Sorption was carried out at room temperature (approximately 22 °C). After the process was completed, the suspension was separated by gravity filtration to separate the solid particles.

The  $Pb^{2+}$  ion content in the tested solutions was determined using an ELMETRON CPI-601 ionometer with a properly calibrated lead-selective electrode.

The efficiency of the  $Pb^{2+}$  ion adsorption process was calculated using the following formula:

$$X = \left( \frac{C_0 - C_k}{C_0} \right) \cdot 100\% \quad (7)$$

where:  $X$  – adsorption efficiency (%),  $C_0$  and  $C_k$  – initial and final concentration of lead ions in solution (mg/dm<sup>3</sup>).

The amount of lead adsorbed by the tested adsorbent, i.e., the sorption capacity, was calculated using the following formula:

$$Q = \frac{V(C_0 - C_k)}{m} \quad (8)$$

where:  $Q$  - amount of lead adsorbed per unit mass of sorbent (mg/g),  $V$  - volume of solution (dm<sup>3</sup>),  $C_0$  and  $C_k$  - initial and final concentration of lead in solution (mg/dm<sup>3</sup>) and  $m$  - amount of dry adsorbent mass (g).

To verify the results of ionometric measurements, additional tests were performed on solutions after the sorption process using an Atomic Absorption Spectrophotometer Thermo Scientific ICE 3500. The detection limit of the spectrophotometer is  $0.2 \cdot 10^{-4}$  mg/dm<sup>3</sup>. A lamp with a hollow cathode made of spectrally pure metal, in this case lead, was used as the radiation source. The lamp emits radiation with a wavelength suitable for analysis. Because only free atoms in their ground state participate in radiation absorption, sample atomization is of significant importance. Atomization was carried out in a gas flame, into which the solution was introduced as an aerosol. The atomiser forms a single unit with the burner. The measurement procedure consisted of introducing the sample solutions into the apparatus and measuring the absorbance. The volume of the solutions intended for testing was approximately 100 ml.

## 3. Results and discussion

### 3.1. Nitrogen adsorption

The specific surface area was calculated using the multipoint Brunauer–Emmett–Teller (BET) method based on the adsorption branch of the nitrogen isotherm. The obtained BET surface areas confirmed substantial differences between the investigated materials: the sunflower husk biochar (SH\_CO<sub>2</sub>) had a surface area of approximately 195 m<sup>2</sup>/g, whereas the cherry stone biochar (CS\_CO<sub>2</sub>) exhibited a markedly higher surface area of approximately 524 m<sup>2</sup>/g. For the biochar obtained in the CO<sub>2</sub> + H<sub>2</sub>O atmosphere, the BET surface area was 679 m<sup>2</sup>/g for sunflower husk biochar and 673 m<sup>2</sup>/g for cherry stone biochar. Additionally, Figure 1 presents the

nitrogen adsorption-desorption isotherms of the obtained biochar, illustrating the differences in adsorption behaviour and pore structure depending on the feedstock type and gasification atmosphere.

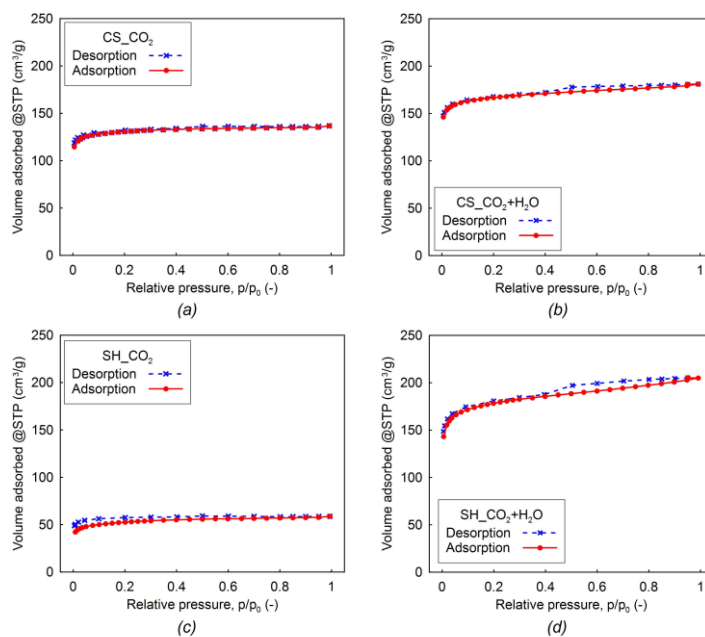


**Figure 1.** Nitrogen adsorption-desorption isotherms of the biochars obtained from cherry stones (CS) and sunflower husks (SH) under CO<sub>2</sub> and CO<sub>2</sub>+H<sub>2</sub>O atmospheres: (a) CS\_CO<sub>2</sub>, (b) CS\_CO<sub>2</sub>+H<sub>2</sub>O, (c) SH\_CO<sub>2</sub>, and (d) SH\_CO<sub>2</sub>+H<sub>2</sub>O.

### 3.2. Phenol adsorption

The adsorption performance was assessed at different initial phenol concentrations (5, 10, 25, and 50 mg/dm<sup>3</sup>) to determine the effect of concentration on adsorption capacity and to better understand the interaction between the adsorbate and the adsorbent. In addition to the equilibrium adsorption capacity ( $q_e$ ), the solution pH after adsorption was measured to assess potential changes in surface chemistry and their influence on adsorption mechanisms. Furthermore, the specific surface area was included in the analysis to examine its relationship with adsorption efficiency.

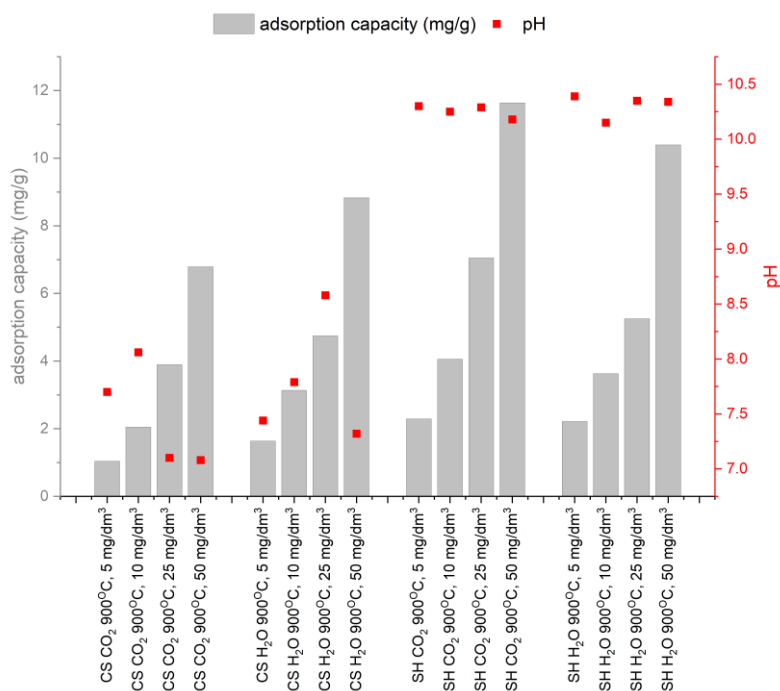


**Figure 1.** Effect of precursor type (cherry stones or sunflower husks), activation method (CO<sub>2</sub>, CO<sub>2</sub>+H<sub>2</sub>O), and initial phenol concentration on adsorption capacity ( $q_e$ ) and solution pH.

The adsorption behaviour of the prepared carbon materials is strongly influenced by the type of biomass precursor (CS or SH), the activation agent (CO<sub>2</sub> or H<sub>2</sub>O), and the initial phenol concentration. As shown in Figure 1, the equilibrium adsorption capacity ( $q_e$ ) consistently increases with increasing initial concentration from 5 to 50 mg/dm<sup>3</sup> for all samples, confirming that a higher concentration gradient enhances mass transfer and promotes more effective occupation of active sites.

A clear distinction can be observed between CS- and SH-derived biochars. The SH-based materials exhibit superior adsorption performance, reaching the highest  $q_e$  values (above 11 mg/g) at 50 mg/dm<sup>3</sup>, particularly for CO<sub>2</sub>-activated samples. In contrast, CS-derived biochars exhibit lower adsorption capacities under comparable conditions, with maximum  $q_e$  values of approximately 7 mg/g for CO<sub>2</sub> activation and 9 mg/g for steam activation. This indicates that sunflower husks are a more favourable feedstock for producing efficient adsorbents for phenol removal.

The effect of the activation agent varies with the feedstock. For CS-based materials, steam (H<sub>2</sub>O) activation leads to improved adsorption performance compared to CO<sub>2</sub> activation, which may be attributed to the development of a more accessible pore structure, including mesopores that facilitate phenol diffusion. On the other hand, SH-based materials achieve the highest adsorption capacities when activated with CO<sub>2</sub>, suggesting that in this case a predominantly microporous structure is more effective for phenol adsorption.

Analysis of the specific surface area ( $S_{BET}$ ) reveals that although higher values are generally associated with improved adsorption performance, there is no direct linear correlation between  $S_{BET}$  and  $q_e$ . For example, CS samples activated with CO<sub>2</sub> exhibit relatively high surface areas but lower adsorption capacities than SH samples, which have slightly lower or comparable  $S_{BET}$  values. This indicates that pore size distribution and surface chemistry play a more decisive role than surface area alone.

The pH values measured after adsorption further supports this interpretation. CS-derived materials maintain near-neutral conditions (pH ~7–8.5), whereas SH-derived carbons exhibit strongly alkaline pH values (~10–10.5). Considering that the pKa of phenol is approximately 10, partial dissociation into phenolate ions occurs in alkaline conditions. Therefore, in the case of SH samples, additional mechanisms, such as electrostatic interactions and specific interactions with surface functional groups, may contribute to enhanced adsorption, alongside  $\pi$ - $\pi$  interactions typical of carbonaceous materials.

To further elucidate the adsorption mechanisms and better understand the role of surface functional groups, additional characterisation using Fourier-transform infrared spectroscopy (FTIR) and X-ray photoelectron spectroscopy (XPS) would be highly beneficial. These analyses are planned for future work and are expected to provide detailed insights into the chemical composition, functional groups, and surface-bonding environments responsible for phenol adsorption.

Overall, the results demonstrate that both the precursor type and activation method significantly affect the physicochemical properties of the adsorbents and, consequently, their adsorption efficiency. Sunflower husk-derived carbons, particularly those activated with CO<sub>2</sub>, show the most promising performance for phenol removal from aqueous solutions.

The equilibrium adsorption data were analysed using the Freundlich, Langmuir, Temkin, and Dubinin–Radushkevich (D–R) isotherm models, and the resulting parameters are summarised in Table 1.

The Freundlich model exhibited the best agreement with the experimental data, particularly for the CO<sub>2</sub>-activated samples (CS\_CO<sub>2</sub> and SH\_CO<sub>2</sub>), with a correlation coefficient ( $R^2$ ) of 0.993. Slightly lower values were observed for the H<sub>2</sub>O-activated samples,  $R^2=0.953$  for CS\_H<sub>2</sub>O and  $R^2=0.920$  for SH\_H<sub>2</sub>O, indicating a somewhat reduced model applicability in these cases. The superior fit of the Freundlich model suggests that the adsorption process occurs on a heterogeneous surface with non-uniform energy distribution.

The Freundlich constant  $K_f$ , associated with adsorption capacity, followed the order: CS\_CO<sub>2</sub> < CS\_CO<sub>2</sub>+H<sub>2</sub>O < SH\_CO<sub>2</sub>+H<sub>2</sub>O < SH\_CO<sub>2</sub>, with values ranging from 0.51 to 3.20 (mg/g)(dm<sup>3</sup>/mg)<sup>1/n</sup>. The highest  $K_f$  value for SH-CO<sub>2</sub> indicates its superior adsorption performance toward phenol. The heterogeneity factor  $n$  ranged from 1.38 to 2.91 for all samples, confirming favourable adsorption conditions ( $n>1$ ) and indicating moderate surface heterogeneity.

The Langmuir model provided a less satisfactory fit ( $R^2 = 0.799 - 0.945$ ), suggesting that the assumption of monolayer adsorption on a homogeneous surface is not fully valid for the studied systems. The maximum adsorption capacity ( $q_m$ ) was similar across all samples, ranging from 10.97 to 12.71 mg/g, indicating comparable adsorption capacities regardless of the activation method.

The Langmuir constant,  $K_L$ , which reflects the affinity between the adsorbate and the adsorbent, was highest for the SH-CO<sub>2</sub> sample (0.24 dm<sup>3</sup>/mg), further confirming its enhanced adsorption efficiency.

The Temkin model showed moderate agreement with the experimental data ( $R^2 = 0.768 - 0.950$ ), indicating that adsorbate-adsorbent interactions contribute to the adsorption mechanism. The Temkin constant  $b_t$ , related to the heat of adsorption, ranged from 1124.81 to 1437.71 J/mol. These relatively low values suggest that the adsorption process is dominated by weak interactions, characteristics of physisorption.

**Table 1.** Parameters of Freundlich, Langmuir, Temkin, and Dubinin-Radushkevich isotherm models for phenol adsorption onto prepared carbon adsorbents.

Models	Parameters	CS_CO <sub>2</sub>	CS_CO <sub>2</sub> +H <sub>2</sub> O	SH_CO <sub>2</sub>	SH_CO <sub>2</sub> +H <sub>2</sub> O
Freundlich	K <sub>f</sub> , mg/g, (dm <sup>3</sup> /mg) <sup>1/n</sup>	0.51	1.36	3.20	2.65
	SE	0.057	0.26	0.17	0.43
	N	1.38	1.93	2.67	2.91
	SE	0.085	0.30	0.19	0.61
	R <sup>2</sup>	0.993	0.953	0.993	0.920
Langmuir	q <sub>m</sub> , mg/g	12.62	11.09	12.71	10.97
	SE	2.15	3.26	2.31	3.89
	K <sub>L</sub> , dm <sup>3</sup> /mg	0.03	0.08	0.24	0.16
	SE	0.01	0.04	0.16	0.16
	R <sup>2</sup>	0.945	0.853	0.938	0.799
Temkin	b <sub>t</sub> , J/mol	1124.81	1134.28	1186.53	1437.71
	SE	183.05	285.54	266.89	558.08
	K <sub>t</sub> , dm <sup>3</sup> /g	0.47	1.10	5.31	4.63
	SE	0.20	0.64	3.20	4.87
	R <sup>2</sup>	0.950	0.853	0.908	0.768
Dubinin–Radushkevich	q <sub>m</sub> , mg/g	4.66	5.99	7.45	6.08
	SE	1.21	1.41	2.04	1.80
	K <sub>DR</sub> , mol <sup>2</sup> /KJ	2.98x10 <sup>-6</sup>	1.05x10 <sup>-6</sup>	1.28x10 <sup>-7</sup>	1.41x10 <sup>-7</sup>
	SE	9.24x10 <sup>-7</sup>	3.47x10 <sup>-7</sup>	5.64x10 <sup>-8</sup>	7.96x10 <sup>-8</sup>
	R <sup>2</sup>	0.839	0.819	0.721	0.610

The Dubinin-Radushkevich (D-R) model exhibited the lowest correlation coefficients ( $R^2=0.610 - 0.839$ ), indicating a poorer fit compared to the other models. The  $K_{DR}$  values were in the order of 10<sup>-6</sup> to 10<sup>-7</sup> mol<sup>2</sup>/kJ<sup>2</sup>, corresponding to low adsorption energies. This further supports the conclusion that the adsorption of phenol onto the studied materials proceeds predominantly via physical adsorption mechanisms rather than chemisorption.

Overall, the adsorption process is best described by the Freundlich model, indicating a heterogeneous adsorption surface and multilayer adsorption behaviour, while thermodynamic considerations derived from the D-R model confirm the predominance of physisorption.

### 3.3. Lead cation (Pb<sup>2+</sup>) adsorption

The adsorption performance toward Pb<sup>2+</sup> ions was evaluated for biochars obtained from sunflower husks and cherry seeds at initial Pb<sup>2+</sup> concentrations of 50, 100, and 150 mg/dm<sup>3</sup>. In addition to the residual metal concentration, the pH and conductivity of the solutions after sorption were monitored in order to gain insight into possible uptake mechanisms.

A pronounced effect of the biomass precursor on Pb<sup>2+</sup> removal was observed. The sunflower husk-derived biochar exhibited exceptionally high sorption efficiency over the entire concentration range studied. In ionometric measurements using a Pb-selective electrode, the residual Pb<sup>2+</sup> concentration after sorption was below the detection limit for all tested initial concentrations, indicating nearly complete removal of lead ions from solution. Verification by atomic absorption spectrometry (AAS) confirmed very low residual Pb<sup>2+</sup> concentrations, ranging from approximately 0.4–0.6 mg/dm<sup>3</sup> and showing no clear dependence on the initial concentration. Due to the high pH of the solution, it can be assumed that the lead was sorbed in the form of hydroxyl ion, such as [Pb(OH)<sub>4</sub>]<sup>2-</sup>. These results demonstrate that sunflower husk biochar is a highly effective sorbent for Pb<sup>2+</sup> and suggest that its adsorption capacity may remain high even at higher inlet concentrations.

In contrast, the cherry seed-derived biochar exhibited markedly lower sorption efficiency, and its performance declined with increasing initial Pb<sup>2+</sup> concentration. Based on ionometric measurements, the sorption efficiency declined from 91.3% at 50 mg/dm<sup>3</sup> to 88.8% at 100 mg/dm<sup>3</sup> and 71.6% at 150 mg/dm<sup>3</sup>. At the same time, the sorption capacity increased from 22.5 to 55.6 mg/g, which is consistent with the higher driving force for mass

transfer at elevated  $Pb^{2+}$  concentrations. Although the AAS/ASA measurements yielded somewhat higher residual  $Pb^{2+}$  concentrations than the ionometric method, both analytical approaches showed the same trend: a progressive deterioration in removal efficiency with increasing initial metal concentration. This indicates that cherry seed biochar may be more suitable for treating solutions with relatively low  $Pb^{2+}$  concentrations.

Changes in the post-sorption solution chemistry further suggest that different adsorption mechanisms operated depending on the precursor type. After contact with sunflower husk biochar, the solution pH increased markedly to strongly alkaline values (approximately 9.7–10.0), and the conductivity also increased substantially. Such behaviour may indicate that, in addition to surface complexation, ion-exchange processes involving inorganic species present in the biochar ash fraction contributed to  $Pb^{2+}$  uptake. In contrast, for cherry seed biochar, the pH remained close to the initial value and the conductivity changed only moderately, suggesting a different balance of mechanisms and a less pronounced contribution of ion exchange.

The observed differences are likely related not only to the textural properties of the materials, but also to their mineral composition and surface chemistry. Surface oxygen-containing functional groups, such as carboxyl and hydroxyl moieties, may participate in  $Pb^{2+}$  binding through electrostatic attraction, surface complexation, and ion exchange. The stronger alkalization and conductivity increase observed for sunflower husk biochar point to a more significant role of mineral constituents and exchangeable ions in lead removal, whereas the lower efficiency of cherry seed biochar may reflect a less favourable surface composition or pore structure for  $Pb^{2+}$  sorption.

Overall, the results confirm that the type of biochar strongly affects the  $Pb^{2+}$  adsorption performance of gasification-derived biochars. Among the investigated materials, sunflower husk biochar showed the most promising behaviour, achieving nearly complete lead removal over the tested concentration range, whereas cherry seed biochar exhibited lower, concentration-dependent efficiency. These findings indicate that sunflower husk-derived carbon materials are particularly attractive as low-cost adsorbents for removing  $Pb^{2+}$  ions from aqueous solutions.

**Table 2.**  $Pb^{2+}$  adsorption performance of biochars derived from sunflower husks and cherry seeds.

Biochar	Initial $C_{Pb^{2+}}$ , mg/dm <sup>3</sup>	Final $C_{Pb^{2+}}$ , ion-selective electrode, mg/dm <sup>3</sup>	Final $C_{Pb^{2+}}$ , ASA, mg/dm <sup>3</sup>	Adsorption efficiency, %	Adsorption capacity, Q, mg/g	pH after adsorption	Conductivity after adsorption, $\mu$ S/cm
SH_CO <sub>2</sub>	50	<0.01	0.61	~100	–	9.99	322
SH_CO <sub>2</sub>	100	<0.01	0.49	~100	–	9.79	272
SH_CO <sub>2</sub>	150	<0.01	0.40	~100	–	9.70	315
CS_CO <sub>2</sub>	50	4.33	6.11	91.3	22.5	5.39	49.0
CS_CO <sub>2</sub>	100	11.2	20.90	88.8	43.1	6.14	84.4
CS_CO <sub>2</sub>	150	42.58	70.55	71.6	55.6	5.89	131.8

## 4. Conclusions

Biochars obtained as solid residues from the gasification of sunflower husks and cherry stones under CO<sub>2</sub> and CO<sub>2</sub> + H<sub>2</sub>O atmospheres exhibited clear potential as low-cost adsorbents for removing both organic and inorganic pollutants from aqueous solutions. The results confirmed that the adsorption performance strongly depended on both the feedstock type and the gasification atmosphere, which influenced the textural properties and surface chemistry of the resulting materials.

For phenol adsorption, sunflower husk-derived biochar exhibited the highest performance, with the SH\_CO<sub>2</sub> sample reaching adsorption capacities above 11 mg/g at the highest initial phenol concentration. Cherry stone-derived biochars were less effective, although the addition of steam improved their adsorption behaviour. The equilibrium data were best described by the Freundlich isotherm, indicating a heterogeneous adsorption

surface and multilayer adsorption behaviour. The relatively low adsorption energy values derived from the Dubinin–Radushkevich model suggest that phenol uptake proceeded predominantly via physisorption. At the same time, the results showed that adsorption efficiency was governed not solely by the BET surface area but also by pore structure and surface chemistry.

For Pb<sup>2+</sup> removal, sunflower husk biochar demonstrated exceptionally high efficiency, achieving nearly complete sorption over the tested concentration range of 50–150 mg/dm<sup>3</sup>. In contrast, cherry stone biochar showed lower and concentration-dependent efficiency, decreasing from 91.3% to 71.6% with increasing initial Pb<sup>2+</sup> concentration. Changes in pH and conductivity after sorption suggested that different uptake mechanisms were involved depending on the precursor type. In the case of sunflower husk biochar, ion exchange and interactions with mineral constituents likely played an important role, whereas cherry stone biochar appeared to rely more on surface-related interactions, with a lower contribution from mineral-assisted mechanisms. It should also be noted that the pH during sorption is extremely important.

Overall, the study demonstrates that gasification-derived biochars from food-industry residues can be successfully valorised as functional sorbent materials. Among the investigated samples, sunflower husk-derived biochars were the most promising for both phenol and Pb<sup>2+</sup> removal. These findings confirm that the solid residues generated during the thermochemical conversion of agro-food waste should not be treated merely as by-products but rather as valuable carbon materials with practical applications in water and wastewater treatment. Further work should focus on detailed surface characterisation and on extending adsorption studies to a broader range of pollutants and operating conditions.

## Acknowledgments

This research was funded in part by the National Science Centre, Poland [Grant no. 2023/51/B/ST8/01531] and by the Ministry of Science and Higher Education, Poland [AGH grant no. 16.16.110.663/501.00-110000-10000]. Research project partly supported by program „Excellence initiative – research university” for the AGH University of Krakow” and textural properties of biochars were carried out using research infrastructure purchased under the “Excellence initiative – research university” programme for AGH University of Krakow.

## References

- [1] Trivedi Y., Sharma M., Mishra R.K., Sharma A., Joshi J., Gupta A.B., Achintya B., Shah K., Vuppaladadiyam A.K., Biochar potential for pollutant removal during wastewater treatment: A comprehensive review of separation mechanisms, technological integration, and process analysis. *Desalination* 2025;600:118509.
- [2] Qambrani N.A., Rahman M.M., Won S., Shim S., Ra C., Biochar properties and eco-friendly applications for climate change mitigation, waste management, and wastewater treatment: A review. *Renew Sustain Energy Rev* 2017;79:255-73.
- [3] Shi X., Ma W., Chen W., Tao X., Gong C., Gao S., Xu L., Fang Z., Enhanced phenol adsorption on Fe-N co-doped biochar: Experimental and simulation insights into the formation mechanism. *Sep Purif Technol* 2026;387:136689.
- [4] Xu T., Gao R., Yan Y., Fang J., Ding S., Application of modified biochar in constructed wetlands for efficient livestock wastewater treatment. *Bioresour Technol* 2025;418:132100.
- [5] Magdziarz A., Korzeniowski Ł., Plata M., Cierpińska M., Mlonka-Mędrala A., Kalemba-Rec I., Jerzak W., Effect of steam-enriched CO<sub>2</sub> atmosphere on the properties of biochar derived from agro-industrial residues gasification. *Book of Abstracts, 20<sup>th</sup> on Sustainable Development of Energy, Water and Environment Systems Conference, 2025*: p. 869.
- [6] Zhang M., Liu R., Huang J., Si W., Wang G., Liu G., Life cycle assessment and environmental benefit analysis of a modified biochar system for heavy metal wastewater treatment. *J Environ Manage* 2025;385:125060.
- [7] Huang W., Bai R., Chen L., Wang X., Li Z., Tian Y., Iron-based lignocellulosic biochar for Fenton-like treatment of organic wastewater: A review on progress and prospects. *Chem Eng J* 2025;511:160678.
- [8] Zhang Z., Li L., Dong H., Pei Z., Aqueous transformation of phenolic pollutants on biochar via dissolved oxygen-driven polymerization. *Water Res* 2025;278:123319.
- [9] Yu H., Liu W., Ling C., Huang G., Shao S., Gui Z., Wang T., Engineering bacterial pretreatment of basswood for enhanced hydrophobicity and phenolic contaminant removal selectivity of derived biochar. *J Hazard Mater* 2025;490:137735.
- [10] Yang R., Liu Q., Liu Z., Wang J., Zhang A., Liu Y., Insights into the Fenton-like degradation efficiency and mechanism of phenolic pollutants by Cu-doped sludge-based biochar catalyst. *Appl Catal B Environ* 2025;386:125336.

- [11] Zhao Z., Yan L., Li G., Rao P., Huo B., Li T., Li Y., Zhang Z., Sun Y., Xue J., Food waste biogas residue-derived composite biochar for effective Cu<sup>2+</sup> removal by capacitive deionization. *J Environ Chem Eng* 2025;13:117132.
- [12] Yapıcıoğlu P.S., Elisa F., Dual benefits on valorization of waste agro-industrial biochar by low-carbon thermal pyrolysis in biochar regeneration for carbon-neutral industrial wastewater treatment and reclaimed water achievement. *J Clean Prod* 2025;503:145857.
- [13] Sieradzka M., Mlonka-Mędrala A., Jerzak W., Magdziarz A., Investigation of environmental advantages of food waste utilization via gasification. *Book of Abstracts, 20th Conference on Sustainable Development of Energy, Water and Environment Systems 2025*, p. 717.